

MULE: A Portable Muon Detection System for Real-Time Subsurface Density Monitoring

筑波大学
University of Tsukuba

ID&E
A member of Tokio Marine Group

Ahmed Ashour¹, Takehiro Takayanagi¹, Keiichi Ota², Kyosuke Yamamoto¹

¹University of Tsukuba, Engineering Mechanics and Energy Department.

²Research & Development Center, Nippon Koei Co., Ltd.

BACKGROUND

Two geohazard-related incidents motivate this study:

CASE 1 (2025 Yashio sinkhole): a deep-seated cavity developed above a sewer pipe over an extended period which was beyond the capabilities of conventional methods (e.g., ground-penetrating radar, in-pipe robotic imaging).

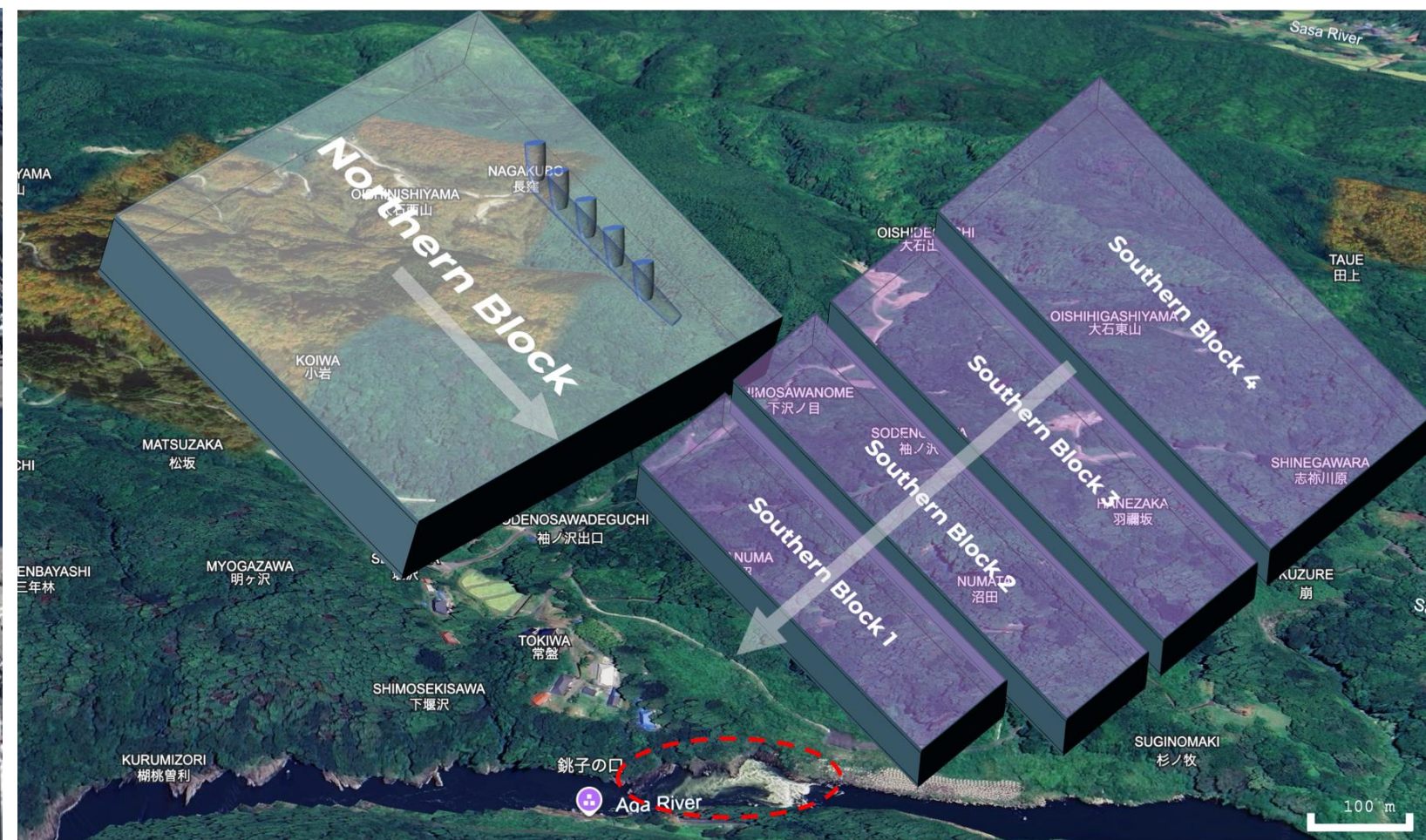
CASE 2 (Takisaka landslide): a historic landslide triggered by saturation levels (due to snowmelt mostly) at failure strata of pumiceous tuff, currently monitored via discrete piezometer points in an existing drainage system.

Both cases raise the similar question: can muography resolve these slow, often localized density changes?

CASE 1



CASE 2



Yashio sinkhole incident (Saitama, Japan) *

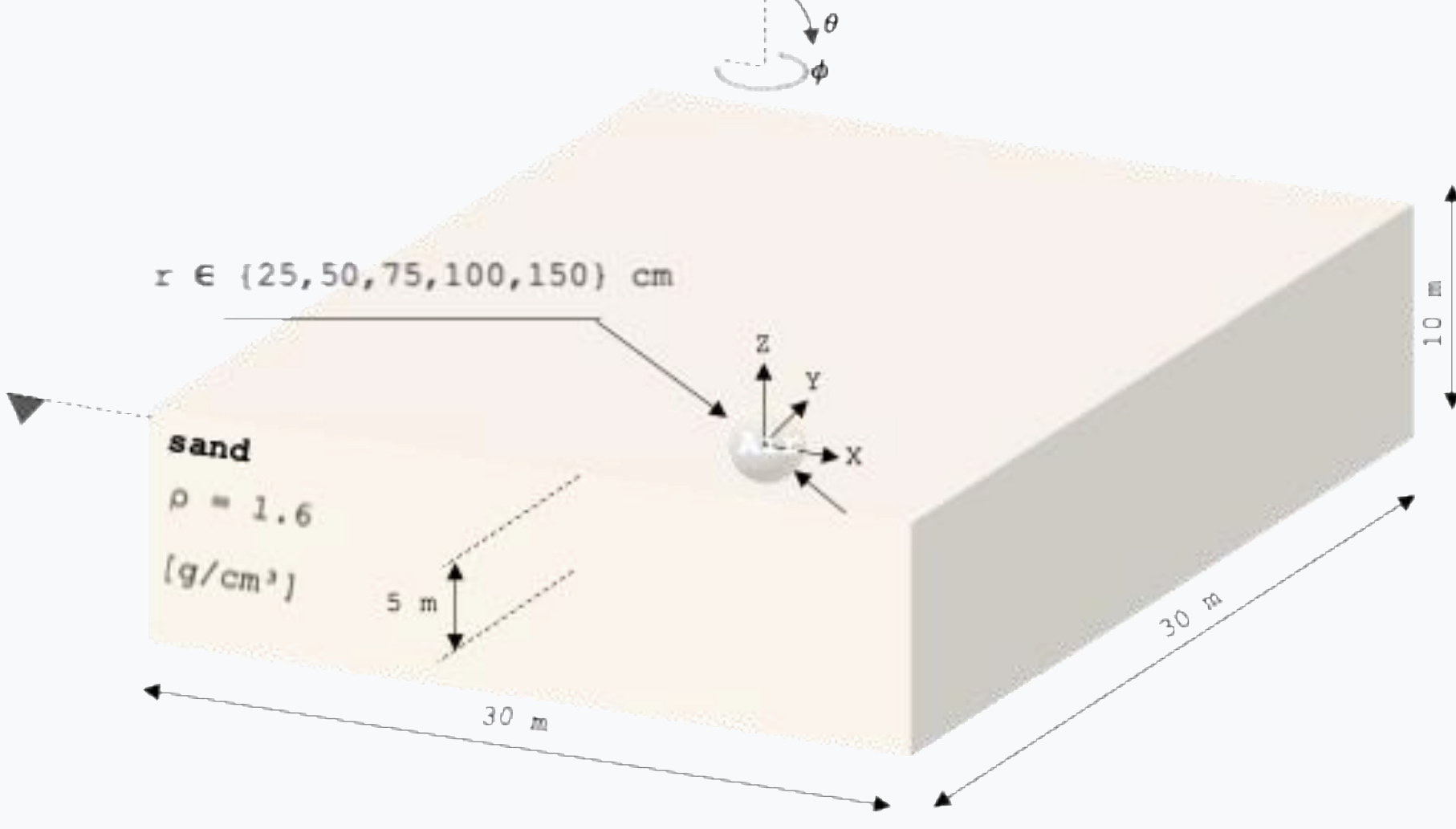
Takisaka landslide area (Fukushima, Japan)

METHODS

CASE 1

Parameter	Value
Target	Sand (SiO ₂)
Target dimensions	30 × 30 × 10 m ³
Cavity geometry	Sphere, r ∈ {25, 50, 75, 100, 150} cm
Cavity depth	5 m (center)
Muon source	E ^{-2.7} , 1-100 GeV, and cos ² (θ)
Zenith range	0-65°
No. of Events	10 ⁷

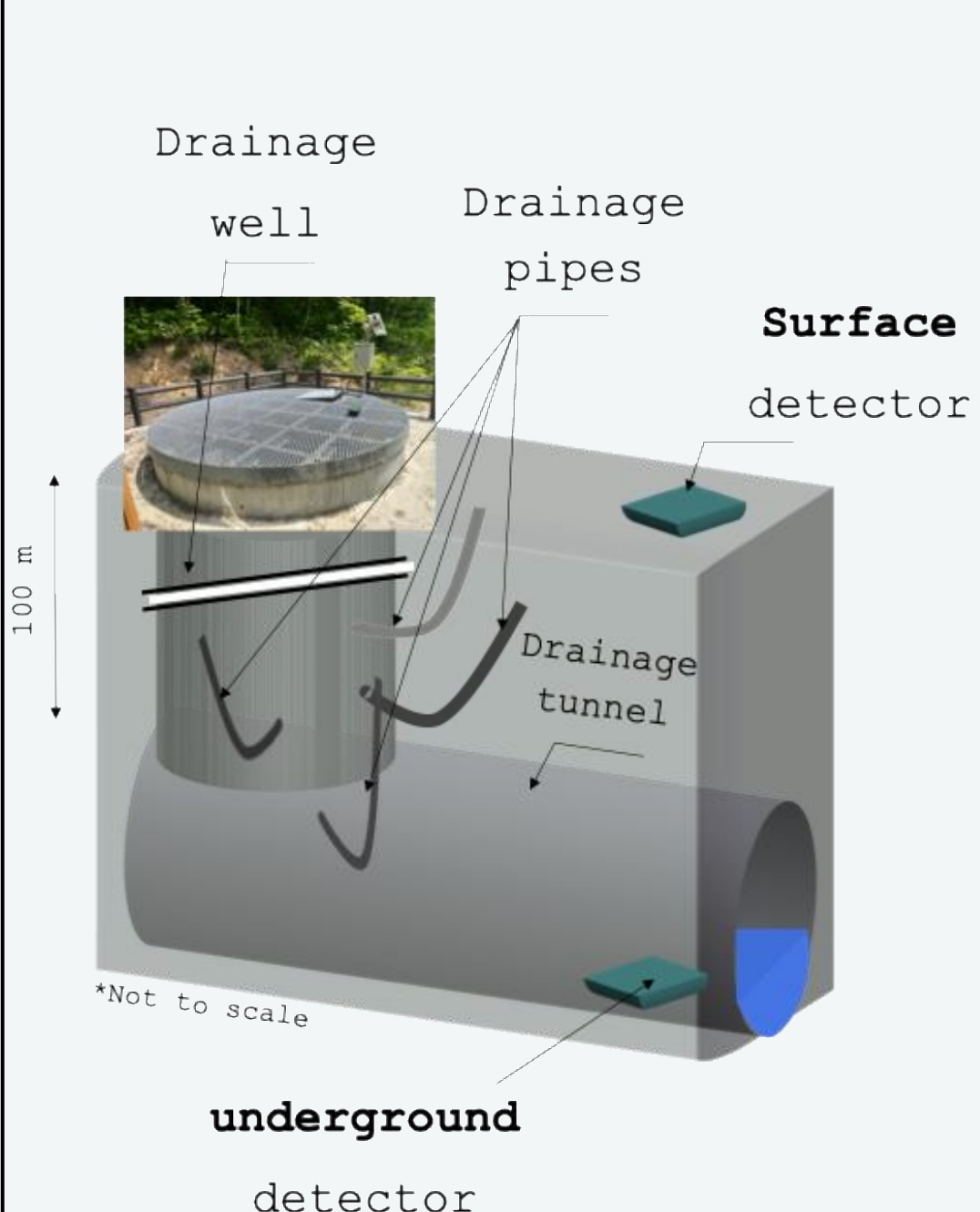
GEANT4 Simulation



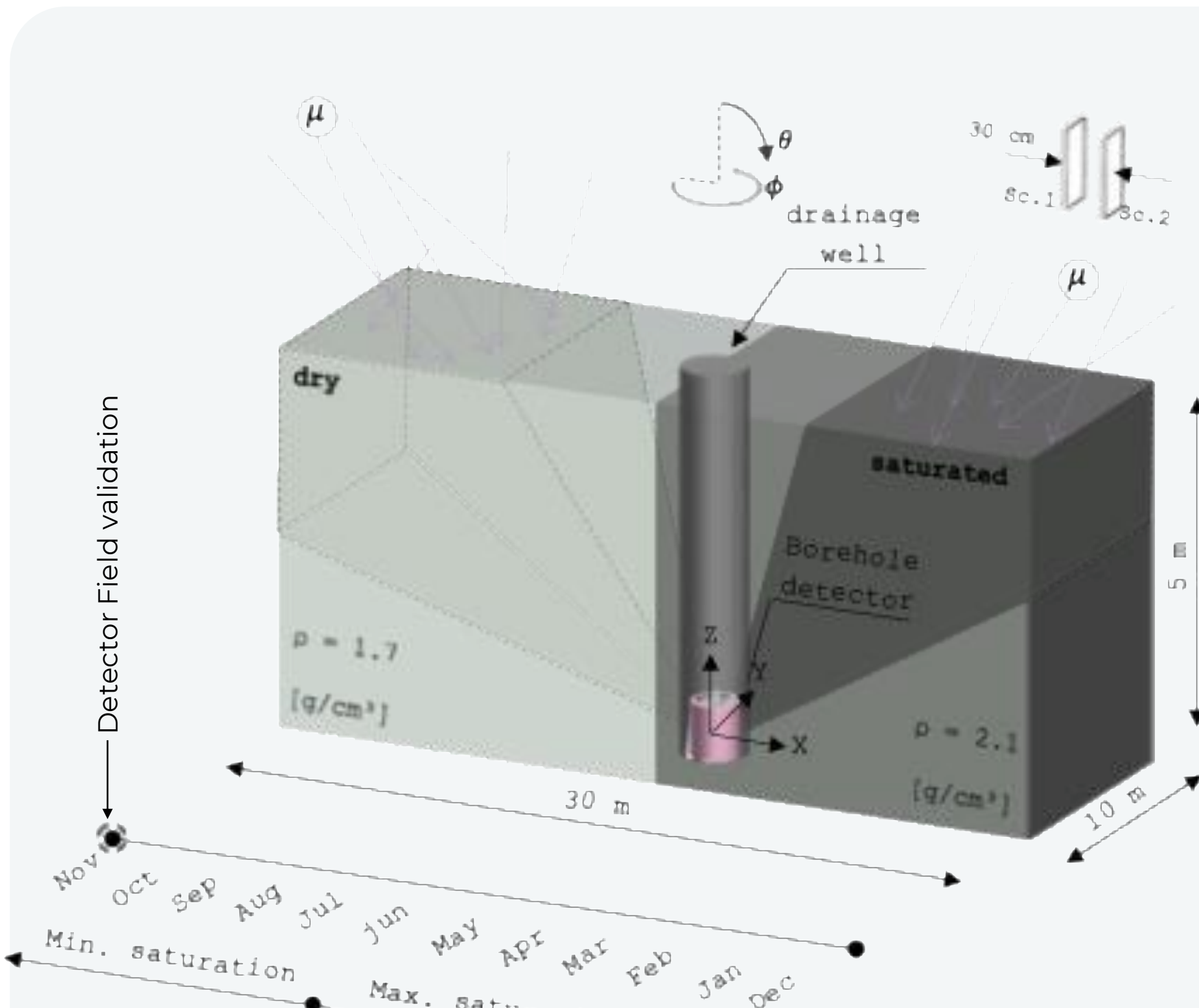
Schematic of target volume for cavity detection (idealized geometry)

CASE 2

Detector field validation



Conceptual deployment in existing drainage infrastructure (Takisaka)



Schematic of target volume for dry/saturated contrast detection (idealized geometry)

CASE 1

A 30 × 30 × 10 m³ slab of sand ($\rho = 1.6 \text{ g/cm}^3$) contains a spherical air cavity at 5 m depth. The cavity radius is varied across a range of $r \in \{25, 50, 75, 100, 150\}$ cm. Detection significance is computed via the projected-trajectory, in which each muon's path is extended to the cavity depth, and survival fractions in the cavity-path region (projected $r < R$) are compared to a surrounding background. Significance is evaluated per zenith bin; the peak σ across bins quantifies detectability at each cavity radius.

CASE 2

A 30 × 10 × 5 m³ split slab contains dry ($\rho = 1.7 \text{ g/cm}^3$) and saturated ($\rho = 2.1 \text{ g/cm}^3$) pumiceous tuff (Si 30%, O 55%, Al 15% by mass; 19% water in the saturated variant). A planar borehole detector (two 25 × 100 cm scintillators, 30 cm gap) embedded at 4.5 m depth. The angular flux anomaly $A(\theta, \varphi)$, fractional deviation from the azimuthal mean at each zenith, is the primary observable. 10⁷ events, 15 – 65° zenith.

A baseline field measurement was performed to establish dry-season detector response in the proposed deployment environment. Two SiPM-based plastic scintillators (~25 cm² effective area each) were stacked as a master/slave coincidence pair at two points within the Takisaka drainage system: a surface site and an underground site with ~100 m overburden. Pulse-height spectra were recorded over ~12 h at each location, normalized to rate density (Hz per ADC bin)

RESULTS

CASE 1

Peak detection significance scales steeply with cavity radius: cavities of radius ≥ 30 cm cross the 3 σ threshold, and $r \geq 50$ cm crosses 5 σ , at 10⁷ events (~5 days exposure on 1 m²). The optimal viewing zenith shifts from ~43° at $r = 25$ cm to ~17° at $r = 100$ cm, reflecting the trade-off between cavity-chord length and cosmic-ray flux. The signal appears in nearly all zenith bins for $r \geq 50$ cm, confirming detection across viewing angles rather than a single-bin fluctuation.

The signal appears in nearly all zenith bins for $r \geq 50$ cm, confirming detection across viewing angles rather than a single-bin fluctuation.

CASE 2

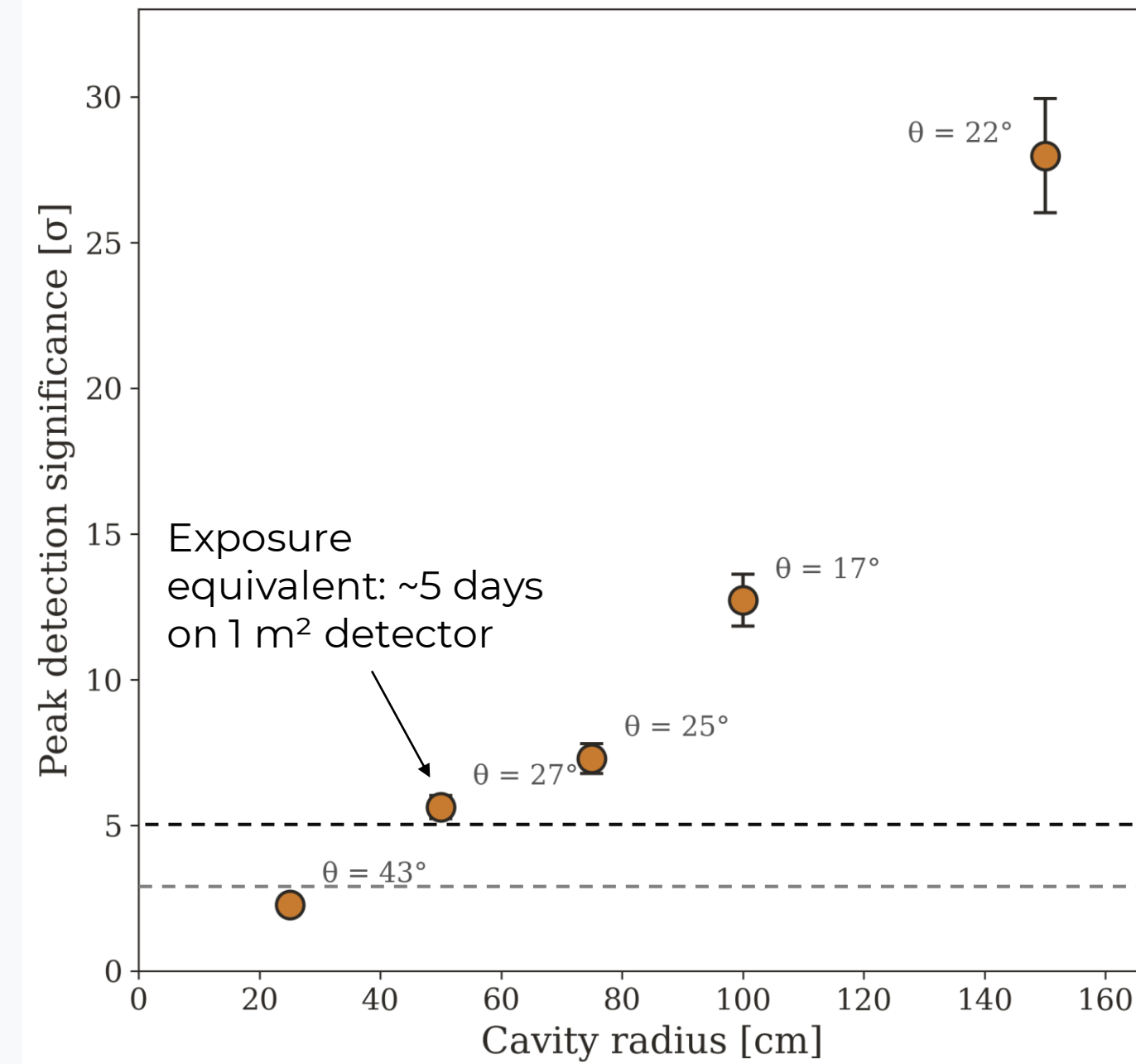
A density contrast of $\Delta\rho = 0.4 \text{ g/cm}^3$ between dry (1.7 g/cm³) and saturated (2.1 g/cm³) pumiceous tuff produces a 35% asymmetry between dry and saturated sides.

The angular anomaly map shows clean azimuthal separation (peak local anomalies +40% dry / -30% saturated); every zenith bin individually exceeds 5 σ , with ratios ranging 1.29-1.41 across 15-65° zenith.

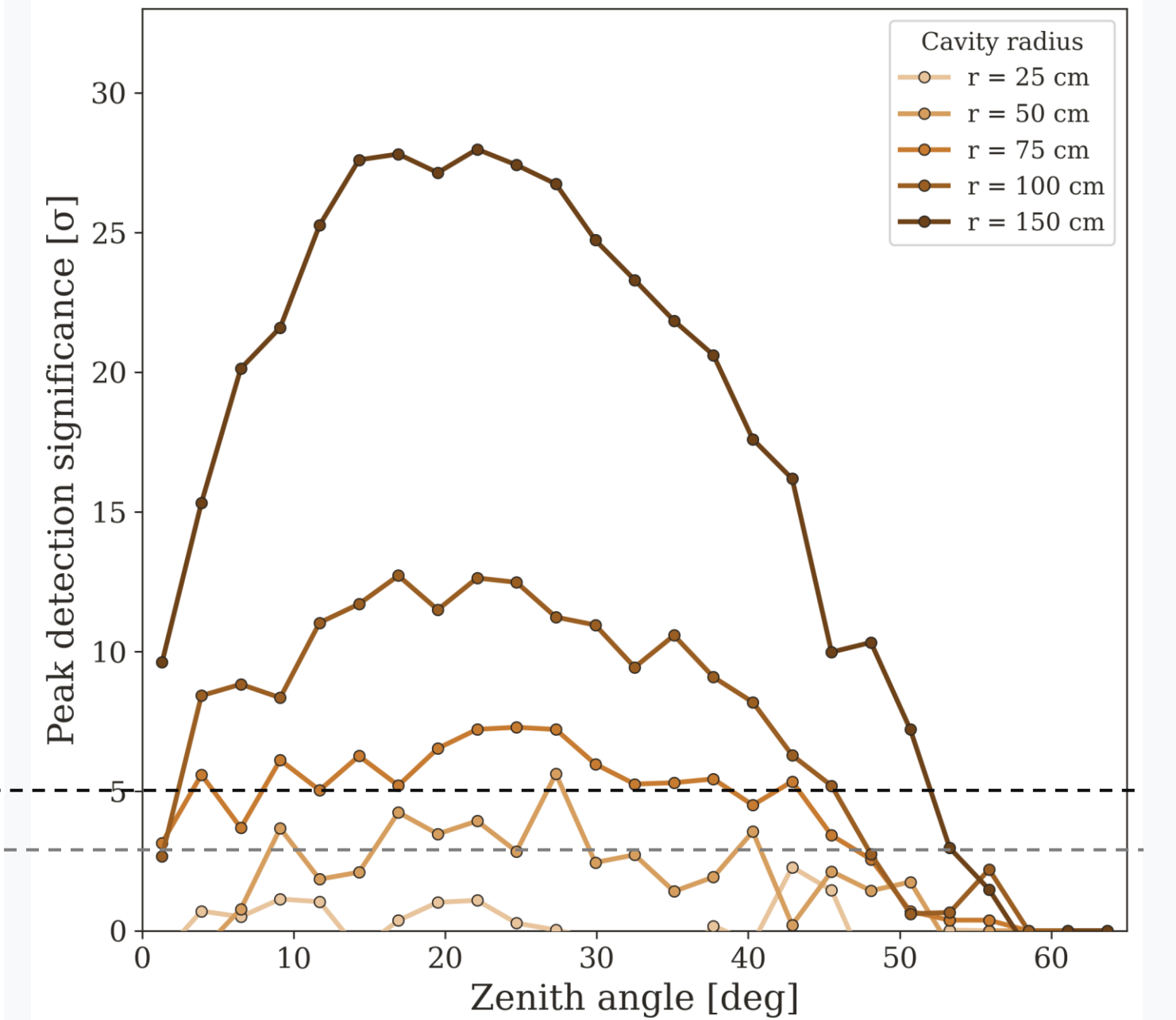
Detector field validation

Coincidence filtering (1 ms window) isolates cosmic muons from backgrounds.

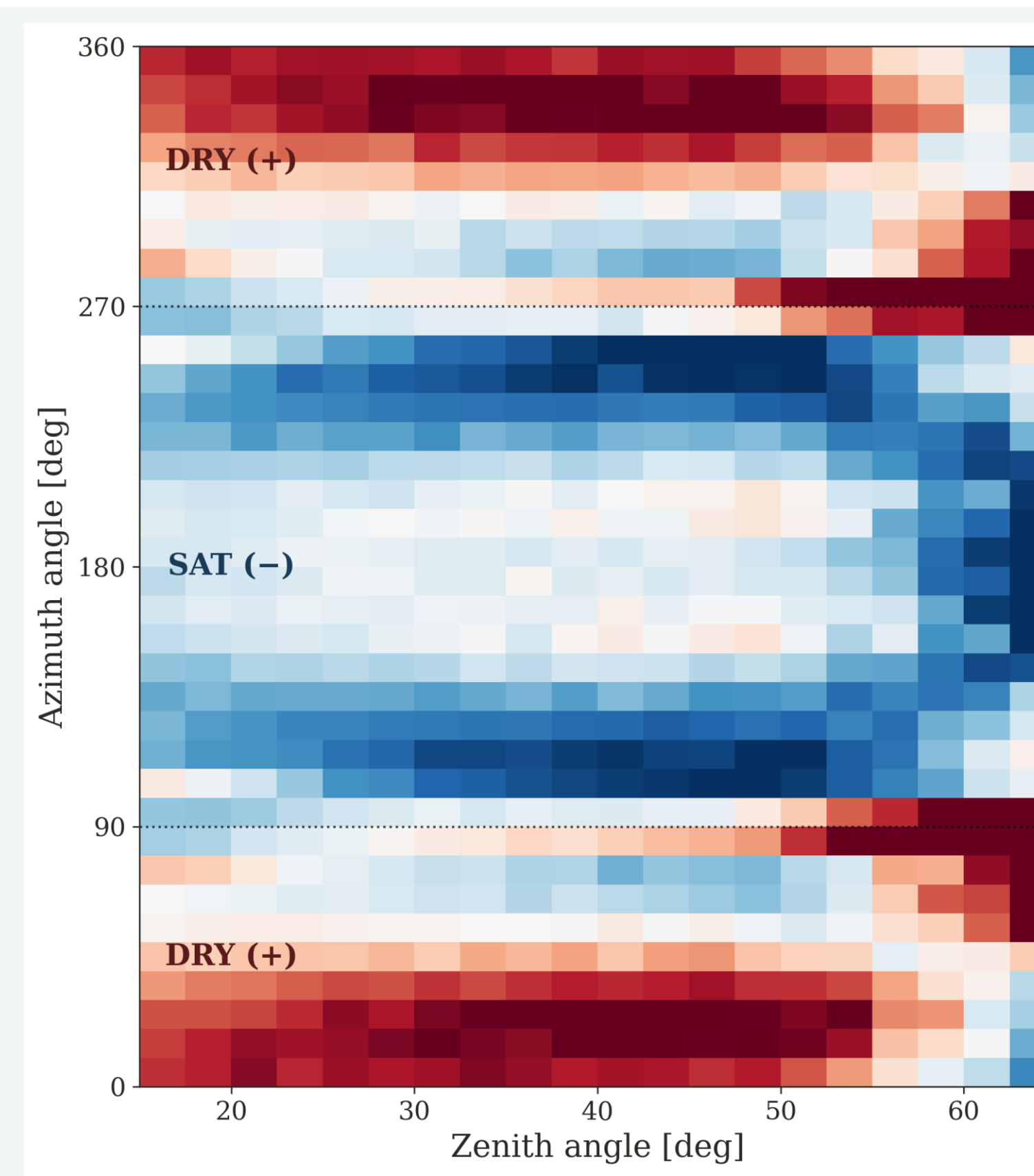
Surface site: 1,663 muon coincidences (S/B ≈ 14 , 12.3 h). Underground site: 27 coincidences (14 h). A dry-season baseline is established at both deployment depths.



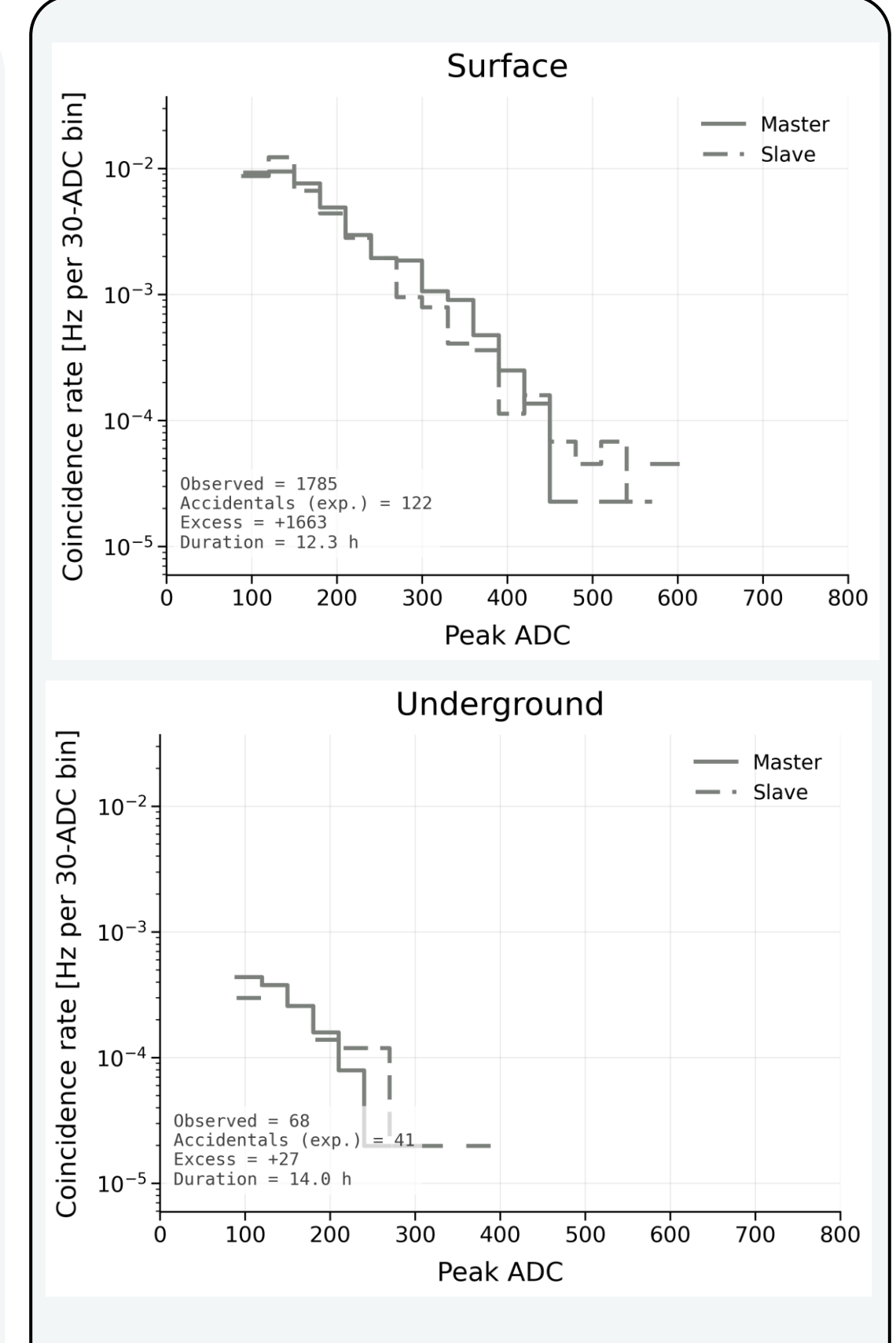
Peak detection significance vs cavity radius



Detection significance vs muon zenith angle



Angular flux anomaly across the split-slab geometry



Prototype field measurements (Nov. 2025)

CONCLUSION & FUTURE WORK

Cavities of radius ≥ 30 cm at 5 m depth in sand are detectable at 3 σ with ~5 days exposure (1 m² detector); saturation contrast in tuff ($\Delta\rho = 0.4 \text{ g/cm}^3$) produces a robust 35% flux asymmetry. Portable scintillator hardware functions at proposed deployment depths. Future work might include (i) explore the depth parameter for CASE 1; (ii) simulate a borehole detector network for CASE 2 to assess spatial coverage; (iii) saturated-season field measurement to observe the seasonal transition. Also, extended the measurement time perhaps with 3-detector stack.

REFERENCES

- 埼玉県. 八潮市で発生した道路陥没事故に関する原因究明委員会 報告書. 埼玉県, 2026.
- “阿賀野川水系 滝坂地区 直轄地すべり対策事業 再評価説明資料,” 北陸地方整備局, 2019.
- H. Shuzui, “Process of slip-surface development and formation of slip-surface clay in landslides in Tertiary volcanic rocks, Japan,” Engineering Geology, vol. 61, no. 4, pp. 199–220, Sep. 2001, doi: 10.1016/S0013-7952(01)00025-4.
- Cimmino, L., Ambrosino, F., Anastasio, A., D’errico, M., Masone, V., Roscilli, L., & Saracino, G. (2021). A new cylindrical borehole detector for radiographic imaging with muons. Scientific Reports, 11(1), 17425.

* Image courtesy Asahi Shinbun